Polymer Journal (2025) 57:897–910
https://doi.org/10.1038/s41428-025-01048-2

ORIGINAL ARTICLE

A deeper dive into primitive polylactate polymerization and microdroplet assembly under restrictive early Earth conditions

Mahendran Sithamparam[1] · Ming-Jing He[2] · Navaniswaran Tharumen[1] · Rehana Afrin[3] · Niannian Ding[3,4] · Chen Chen[5] · Ruiqin Yi[6] · Po-Hsiang Wang[2,7] · Tony Z. Jia[3,8] · Kuhan Chandru[1,9,10]

Received: 23 January 2025 / Revised: 2 April 2025 / Accepted: 15 April 2025 / Published online: 30 April 2025
© The Author(s) 2025. This article is published with open access

Abstract

Alpha hydroxy acids (AHAs) play various roles in modern biology such as in metabolism, but could have played different roles as "non-biomolecules" at the origins of life. Specifically, lactic acid (LA) and other AHAs can polymerize into polyesters and subsequently assemble into membraneless microdroplets (MMDs) upon dehydration-rehydration cycles, suggesting that polyester MMDs could have been relevant protocell models on early Earth. However, in particular, how the harsh conditions of early Earth, namely salinity and decreased reactant volume/concentration, could have affected primitive LA polymerization and subsequent MMD assembly is unclear. In this study, we found that while monovalent salts such as NaCl and KCl did not inhibit LA polymerization and MMD assembly even at high concentrations (up to 1 M), divalent salts such as $MgCl_2$ and $CaCl_2$ were inhibitory at much lower concentrations. Additionally, we found that lower reaction volumes and concentrations, potentially simulating confined microenvironments on early Earth, still supported LA polymerization and MMD assembly to some extent, albeit with decreased efficiency. These results suggest that early Earth's environmental conditions could have still supported the polymerization of LA and the formation of MMD-based protocells in a variety of settings despite being quite harsh and variable.

Introduction

Non-biomolecules, a class of molecules that are either not present to a high degree or do not maintain the same role as in modern biology, are proposed to have played a key role in the chemical evolution leading to the origin of life (OoL)

These authors contributed equally: Mahendran Sithamparam, Ming-Jing He, Navaniswaran Tharumen

Supplementary information The online version contains supplementary material available at https://doi.org/10.1038/s41428-025-01048-2.

✉ Po-Hsiang Wang
pohsiang@ncu.edu.tw

✉ Tony Z. Jia
tzjia@elsi.jp

✉ Kuhan Chandru
kuhan@ukm.edu.my

[1] Space Science Center (ANGKASA), Institute of Climate Change, National University of Malaysia, Bangi, Selangor 43650, Malaysia

[2] Graduate Institute of Environmental Engineering, National Central University, No. 300, Zhongda Road, Zhongli District, Taoyuan City 320, Taiwan

[3] Earth-Life Science Institute, Institute of Science Tokyo, 2-12-1-IE-1 Ookayama, Meguro-ku, Tokyo 152-8550, Japan

[4] China University of Geosciences, Xueyuan Road 29, Haidian District, Beijing 100190, China

[5] Biofunctional Catalyst Research Team, RIKEN Center for Sustainable Resource Science (CSRS), 2-1 Hirosawa, Wako, Saitama 351-0198, Japan

[6] State Key Laboratory of Deep Earth Processes and Resources, Guangzhou Institute of Geochemistry, Chinese Academy of Sciences, Guangzhou 510640, China

[7] Department of Chemical Engineering and Materials Engineering, National Central University, No. 300, Zhongda Rd., Zhongli District, Taoyuan 32001, Taiwan (R.O.C.)

[8] Blue Marble Space Institute of Science, 600 1st Ave, Floor 1, Seattle, WA 98104, USA

[9] Polymer Research Center (PORCE), Faculty of Science and Technology, National University of Malaysia, Bangi, Selangor 43600, Malaysia

[10] Institute of Physical Chemistry, CENIDE, University of Duisburg-Essen, 45141 Essen, Germany

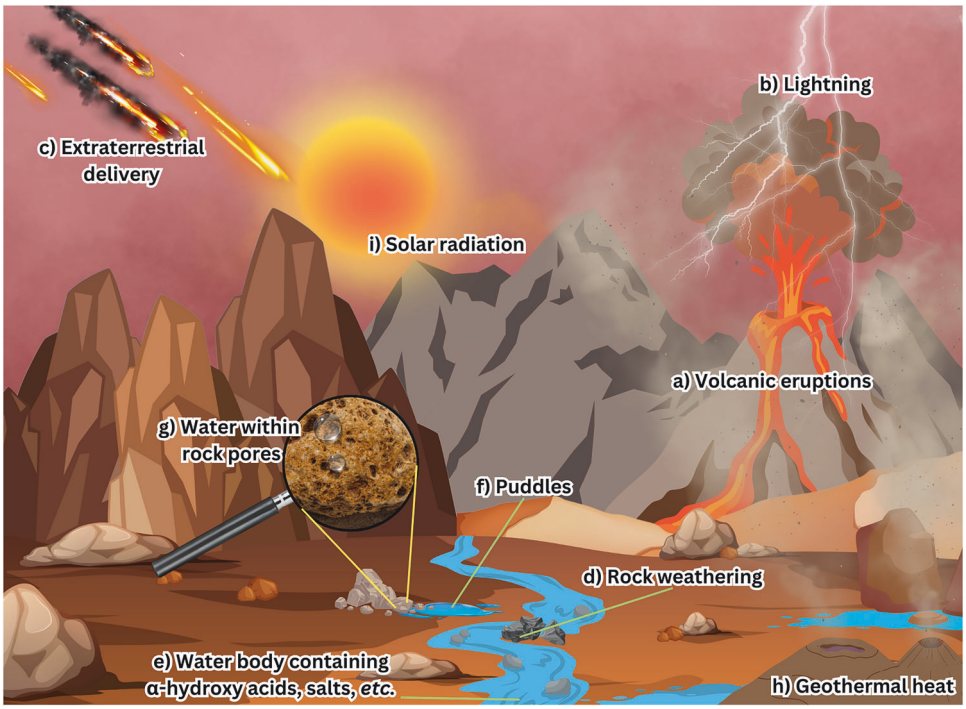

Fig. 1 Illustration of possible prebiotic environments on early Earth relevant to AHA-related chemistries. These phenomena and conditions include **a** volcanic eruptions, a possible source of AHAs and mineral-rich substrates; **b** lightning, potentially driving the abiotic synthesis of AHA molecules through high-energy spark discharges; **c** extraterrestrial delivery of carbonaceous meteorites as a source of AHA and salts; **d** rock weathering, leading to the leaching of minerals, releasing salts into streams, rivers, and oceans; **e** primitive water bodies, serving as reservoirs for dissolved AHA and salts; **f** puddles, which could exist from ebb and flow of water and facilitate cycles of hydration–dehydration critical for polymerization reactions; **g** magnified view of rock pores to emphasize their possible role as localized micro-environments for prebiotic AHA polymerization; **h** geothermal heat; and **i** solar radiation, which possibly could provide the energy required for prebiotic polymerization reactions

[1–4]. One such so-called "non-biomolecule" is the alpha-hydroxy acid (AHA), which is structurally similar to alpha-amino acids and was likely available on early Earth as a result of terrestrial spark discharge [5, 6], ultraviolet irradiation reactions [7], hydrothermal reactions [8], or extraterrestrial deliveries *via* carbonaceous meteorites [9, 10]. AHAs can then polymerize into polyesters through dehydration synthesis *via* heating under mild temperatures, mimicking the dry phase of wet-dry cycles [11–13]; dehydration reactions with both AHAs and alpha-amino acids produce depsipeptides [14], a proposed primitive precursor to peptides. Upon aqueous rehydration, the resulting gel-like polyesters then assemble into membraneless compartments in the form of microdroplets due to phase separation [15]. These membraneless microdroplets (MMDs), with their unique localized polymeric components, can segregate various chemicals (e.g., nucleic acids, salts, or small molecule dyes) [16, 17], suggesting their plausible role in chemical evolution and as protocells [15, 18, 19].

While the polymerization of AHAs are a prerequisite for the formation of MMDs in primitive environments, environmental conditions on early Earth, such as extreme temperatures (e.g., volcanic heat) [20], high salinity [21–24], fluctuating pH (e.g., acidic or alkaline pools) [25, 26], high pressures (e.g., deep-sea environments) [27, 28], or exposure to intense solar radiation (e.g., ultraviolet light) [29], could significantly influence, disrupt, or even completely inhibit AHA polymerization and subsequent MMD assembly.

In particular, salts were highly abundant on early Earth [30, 31] and were produced through processes such as hydrothermal activity [32], volcanic activity [33], and serpentinization [34]. Thus, it is plausible that the potential high concentration of salts in a variety of primitive environments on early Earth could inhibit or at least affect AHA polymerization or subsequent MMD assembly. Furthermore, various types of aquatic environments, ranging from vast oceans to small and transient water bodies such as pores at the ocean, river banks and deltas, cavities within rocks, shallow pools, puddles, and tidal flats [35] could have existed on early Earth (Fig. 1). Smaller and more confined environments could facilitate localized high concentrations of reactive molecules, enhancing the likelihood of molecular bonding and polymerization [36]. In contrast, larger, more dilute environments might have hindered these processes due to lowering concentration of AHA reactants.

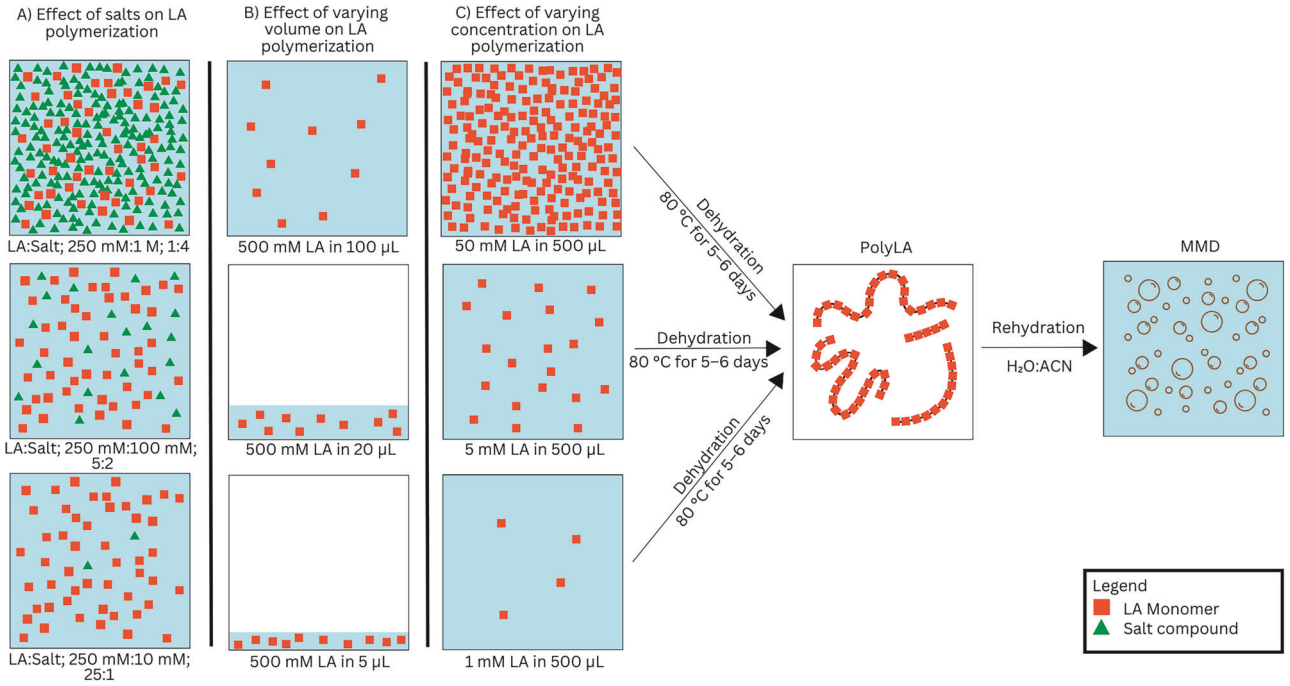

Fig. 2 A block diagram showing the conditions tested in this study. Effects of **A** salts and their concentrations, **B** volume constraints, and **C** varying LA concentrations on LA polymerization and MMD formation. The dehydration was performed at 80 °C for 5–6 days, yielding polyLA. Subsequent rehydration in H_2O: ACN transitions polyLA into MMDs, highlighting the critical role of concentration, ionic conditions, and volume in facilitating prebiotic polymerization and droplet formation

For instance, small water bodies (e.g., tide pools or geothermal pools) or being within porous rocks could concentrate the AHA monomers and facilitate polymerization, overcoming the dilution effects prevalent in larger bodies of water. Thus, whether AHA polymerization and subsequent MMD assembly could still occur within such confined or dilute conditions remains only minimally explored [37].

Previously, we found that the polymerization and subsequent MMD assembly of phenyllactic acid (PA), an AHA that shows robust primitive synthesis and MMD assembly properties, may be hindered at lower reactant volumes and concentrations and at higher concentrations of divalent salts, i.e., 100 mM $CaCl_2$ (somewhat suppressed polymerization) [16] and 1 M $MgCl_2$ (complete inhibition of polymerization) [37], but not monovalent salts such as NaCl and KCl even at concentrations as high as 1 M [16, 37]. Based on these findings, we speculated that increasing the salt concentration and decreasing the reaction volume and concentration could hinder AHA polymerization and MMD assembly in general. We thus extend our previous studies to probe lactic acid (LA) polymerization under similar extreme early-Earth conditions as a proxy representative AHA to investigate primitive polyester polymerization and subsequent MMD assembly more generally. We specifically chose LA due to its simple structure, plausible ubiquity, and stability on early Earth, as PA may not be as prebiotically plausible as LA (PA contains more than eight carbon molecules and larger molecules are considered less prebiotically plausible [38, 39]), and its robustness in relevant prebiotic polymerization and MMD assembly studies performed by our lab to-date [12, 15, 17, 40, 41]. For instance, LA is reported to have existed in carbonaceous chondrites (e.g., Ryugu) [42, 43], detected in Miller–Urey–type spark discharge reaction products [6], and derived from the decomposition of polycyclic aromatic hydrocarbons from anoxic sulfur-rich atmospheres and iron-rich dust [44] and hydrothermal vents on early Earth [8]. The photoactivity of LA under ultraviolet-C radiation from the prebiotic Sun also demonstrates its stability in such environments, further supporting its potential presence and persistence during Earth's early stages [16, 45].

In this study, we probed LA polymerization at 80 °C (typically used in previously published studies) and subsequent MMD assembly in the presence of NaCl, KCl, $MgCl_2$, and $CaCl_2$ at concentrations of up to 1 M (Fig. 2). We specifically chose these chloride salts due to their abundance in modern seawater (0.4–0.5 M [46], 10 mM [47], 50 mM [47], and 10 mM [46], respectively), their potential availability in ancient water bodies [48], icy moons [49, 50], their roles in prebiotic chemistry [51–53], and their relevance in modern biology, which may indicate their function at the origins of life. Specifically, monovalent ions such as Na^+ and K^+ maintain electrochemical gradients across cellular structures [54, 55] and could have been crucial for early molecular interactions and the development of primitive cellular structures. Similarly,

divalent ions such as Mg^{2+} and Ca^{2+} could have been important players in primitive nucleic acid polymerization/function [56] or structural integrity and assembly of early molecular systems due to their ability to facilitate gel formation and crosslinking [57–59]. To simulate small-scale aqueous microenvironments, we also investigated LA polymerization and subsequent MMD assembly at reduced volumes down to 5 µL and at reduced reactant concentrations down to 1 mM (Fig. 2). These findings highlight the necessity of balancing localized concentration and volume effects with environmental constraints such as salinity to understand how primitive AHA polymerization and polyester assembly processes might have occurred under more realistic prebiotic settings and for more than just one type of AHA in general.

Materials and methods

Chemicals

DL-Lactic acid (LA) was purchased from Sigma-Aldrich (St. Louis, MO, USA). Acetonitrile (ACN) was purchased from Merck (Darmstadt, Germany) or Tokyo Chemical Industry (Chuo-ku, Tokyo, Japan). All salts (sodium (NaCl), potassium (KCl), calcium (dihydrate) ($CaCl_2$), and magnesium (hexahydrate) ($MgCl_2$) chlorides) were purchased from Nacalai Tesque (Kyoto City, Kyoto, Japan). Ultrapure water was produced by a Barnstead™ Smart2-Pure™ water filtration system (Thermo Fisher Scientific, Waltham, MA, USA).

Synthesis

We prepared stock solutions of LA by dissolving an appropriate amount of LA in ultrapure water to produce a final 500 mM concentration; this stock solution was used for all synthesis experiments. 2 M, 200 mM, and 20 mM stock solutions of each salt were also prepared by dissolving each salt in ultrapure water. Without adjusting pH, the LA stock solution was then diluted to the appropriate concentration (or used without dilution), and the appropriate volume was transferred into a 1.5 mL Eppendorf tube (Hamburg, Germany), followed by the addition of the relevant salt stock solution (if applicable). This tube was then heated to complete dryness at 80 °C for 5–6 days with the cap open in a dry bath (Sahara 310 or Sahara 320, Rocker Scientific, New Taipei City, Taiwan) in a draft chamber. In detail, for experiments in the presence of salts, 250 µL of 500 mM LA was added to 250 µL of the respective salt stock solution (2 M, 200 mM, or 20 mM), leading to a final salt concentration of 1 M, 100 mM, and 10 mM, respectively. For experiments varying LA concentration, 500 µL of the appropriate LA stock solution (500 mM, 50 mM, 5 mM, or 1 mM) was used. For experiments varying LA volume, 500 µL, 100 µL, 20 µL, or 5 µL of the 500 mM LA stock solution was used.

MALDI sample preparation and analysis

We subjected the synthesized polyester samples to positive MALDI-Time of Flight (ToF)-MS analysis through the Institute of Science, Tokyo (formerly Tokyo Institute of Technology) Materials Analysis Division (ultrafleXtreme Bruker Daltonics, Billerica, MA, USA; external mass calibration was performed by the user facility using standard peptide mixtures). The facility first dissolved samples in 9:1 tetrahydrofuran (THF):water (samples with salt) or pure THF (samples without salt) to 10 mg/mL if the sample mass was known. If the sample mass was unknown, the sample was dissolved in a total of 100 µL of 9:1 THF:water or THF. DCTB (3-(4-tert-butylphenyl)-2-methyl-2-propenylidene malononitrile) and CHCA (alpha-cyano-4-hydroxy-cinnamic acid) were used as sample matrices for all samples. DCTB or CHCA was then dissolved in THF to 10 mg/mL and then mixed with each sample (10:1 (v/v)), followed by application to the MALDI plate and subsequent analysis. We acquired each sample in singlicate in each matrix, leading to each sample being analyzed in duplicate on aggregate.

Monoisotopic peaks were then identified by isolating the highest intensity peak in an isotope envelope corresponding to a polymer product using a peak list generated from the mMass software (Open Source Software, Prague, Czech Republic). Major peaks were isolated by applying the following parameters: S/N > 10, absolute peak intensity >1000, and baselining (100 precision and 0 relative offset). Mass accuracy in ppm was calculated by comparing the observed mass with the calculated mass for major peaks corresponding to polymerization products. The intensities of all spectra peaks were plotted and normalized as follows. The Δ72.06 Da mass ladder observed between adjacent peaks serves as clear evidence of LA polymerization resulting from water loss occurring during the polymerization process. We normalized each spectrum based on the intensity of the highest peak observed across all conditions in the same set of experiments (salt: 10 mM, 100 mM, and 1 M; concentration: 10 mM, 100 mM, and 1 M; volume: 5 µL, 20 µL, and 100 µL) using the same matrix. For example, in the set of variable NaCl salt concentration experiments using CHCA, the highest intensity peak was observed in the 1 M NaCl + 250 mM LA reaction, and thus spectra containing 100 mM and 10 mM of NaCl using CHCA matrix were also normalized based on this peak intensity. Detailed peak lists are presented in the Supporting Information.

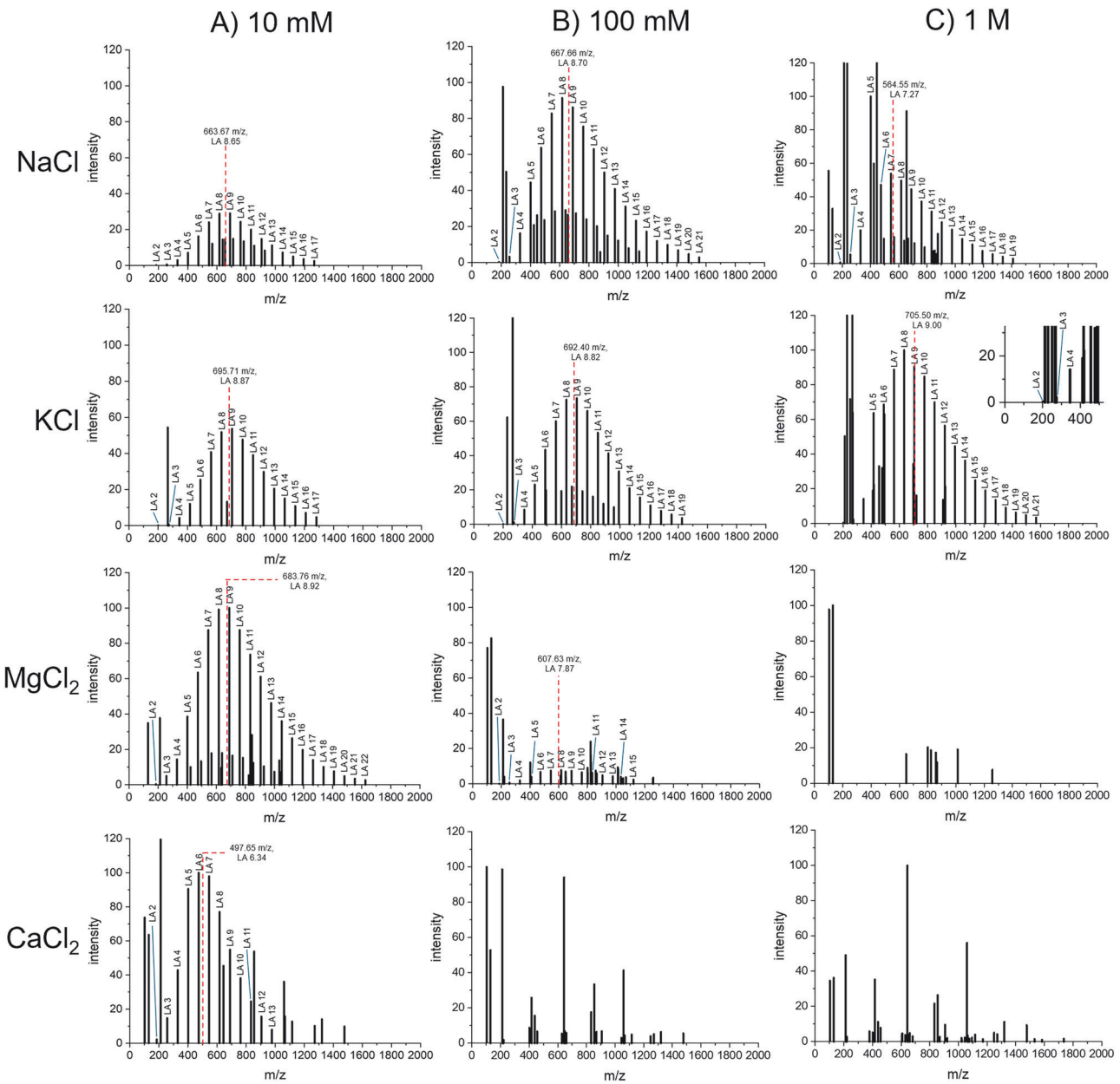

Fig. 3 Comparison of MALDI-ToF-MS spectra (CHCA matrix) of LA synthesis under varying concentrations of **A** 10 mM, **B** 100 mM, and **C** 1 M of different salts, which are NaCl, KCl, $MgCl_2$, and $CaCl_2$. No polymers were detected in 1 M $MgCl_2$, 100 mM $CaCl_2$, or 1 M $CaCl_2$. The estimated center of mass (m/z) and length (mers) of polyLA products measured for each spectrum are denoted by thin red dashed lines. Peaklists of these spectra with evidence of polyLA formation are presented in Supplementary Tables S1–S9. Similar results were observed in MALDI-ToF-MS spectra using DCTB as the matrix, which are presented in Supplementary Fig. S1 along with their peaklists in Supplementary Tables S10–S18

Center of mass estimation

We estimated the center of mass (the polymer length and size where the summed sodiated polymer peaks below the center of mass are equal to those above) of all spectra using a previously published semi-quantitative method [41]. This estimation does not take into account unreacted monomers or other adducts, and because MALDI is not inherently quantitative in the absence of intensity standards, this estimation is simply a semi-quantitative approximation; the precise center of mass may be slightly different than estimated.

In particular, all sodiated polymer peak intensities for each sample were summed (I_{total}). For a polymer of length n (P_n), the intensities of all sodiated polymer peaks below and equal in mass to the peak representing P_n were also summed (I_n). I_n/I_{total} was then calculated as the fractional spectral mass intensity below and including the peak representing P_n. The peak where I_n/I_{total} exceeds 0.5 was estimated as the

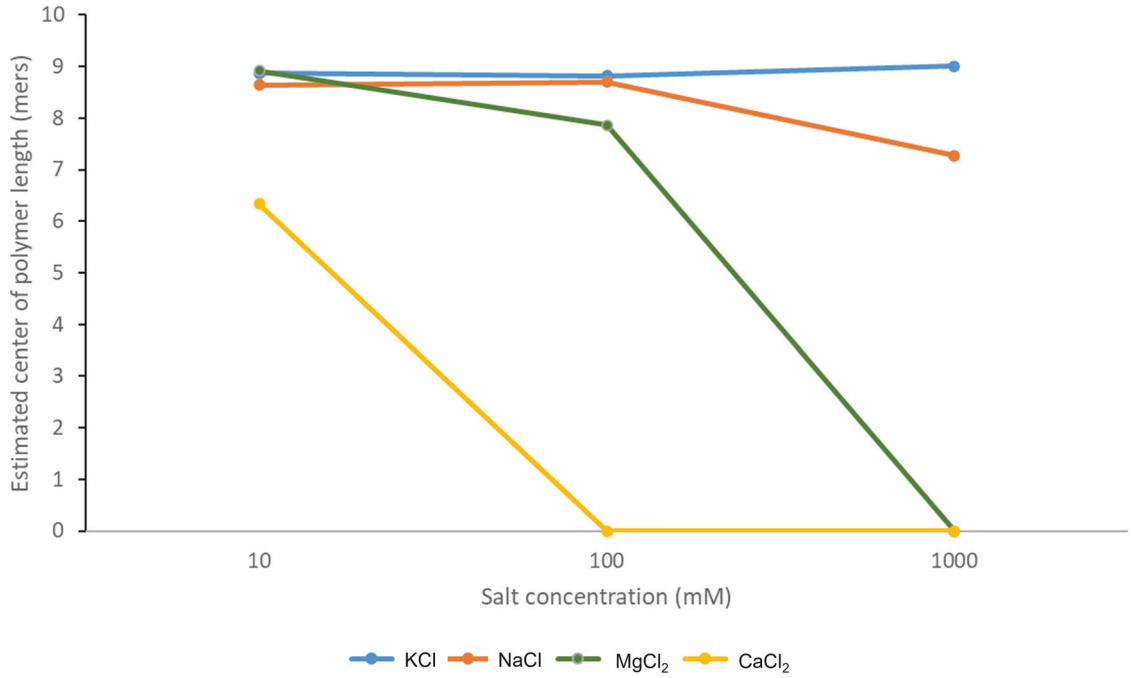

Fig. 4 The estimated center of polymer length (in mers) as a function of salt concentration (10, 100, and 1000 mM) for KCl, NaCl, $MgCl_2$, and $CaCl_2$. The values are derived from the polymer length distribution obtained through spectral analysis, reflecting the effect of each salt on polymerization; the values are presented in Supplementary Table S19

approximate "center of mass". A more accurate center of mass was then calculated by subtracting the fractional offset value $72.0211*(I_n/I_{total} - 0.5)/[(I_n - I_n)/I_{total}]$ from the mass of the peak representing P_n (72.0211 represents the mass difference between adjacent polymer peaks), as well as by subtracting the fractional offset value $(I_n/I_{total} - 0.5)/[(I_n - I_n)/I_{total}]$ from n.

Microscopy

We first hole-punched strong-type double-sided tape (Naisutakku, Nichiban KK, Tokyo, Japan) and applied it to a glass slide (76 mm × 26 mm × 1 mm; Marienfeld Glass, Lauda-Königshofen, Germany or Matsunami Glass, Kishiwada-shi, Osaka, Japan). We then rehydrated the polymer samples after synthesis (directly in the Eppendorf tube) with 4:1 (v/v) water:ACN. For all samples containing salt, the rehydration volume was 500 µL. For samples with varying volume (500 µL, 100 µL, 20 µL, and 5 µL), the rehydration volumes were 500 µL, 100 µL, 20 µL, and 20 µL, respectively. For samples with varying concentrations (500 mM, 50 mM, 5 mM, and 1 mM), the rehydration volumes were 500 µL, 50 µL, 20 µL, and 20 µL, respectively. In some cases, due to overcrowding of droplets (especially for extremely low-volume or high-concentration samples), the rehydration volume was increased to 50–100 µL. After rehydration, we vortexed the sample and added 2.5 µL of each sample to the vacated area within the tape on the glass slide. We then covered the sample with a glass coverslip (22 × 22 mm, Marienfeld Glass or No. 1 18 × 18 mm, Matsunami Glass). Brightfield microscopy images were acquired using a ZEISS AXIOSKOP 2 microscope (Carl ZEISS AG; Oberkochen, Germany) equipped with a 40×/0.75 Plan-Neofluar objective or on a DM5500 B upright epifluorescence microscope (HC PL FLUOTAR 40×/0.80 PH2 air objective, Leica, Wetzlar, Germany). Images were analyzed with a ZEISS ZEN microscope or Leica LAS X software and analyzed using FIJI (Fiji is Just ImageJ, http://fiji.sc).

LA evaporative loss estimations

500 µL of a 500 mM L-LA solution was subjected to dehydration synthesis at 80 °C over seven days. The resulting product gel dry weights (9.6 mg, 9 mg, and 10.7 mg) were obtained and compared to the theoretical L-LA mass of 22.5 mg, with a calculated loss of 56.7 ± 3.8%.

Results and discussion

Influence of salt on the synthesis of LA polymers

Understanding the influence of salts on the AHA-polyester gel system is crucial for elucidating saline conditions that could facilitate, hinder, or catalyze prebiotic polymerization processes on Earth or even other watery planets. Our recent study reported that the polymerization of PA can still occur in

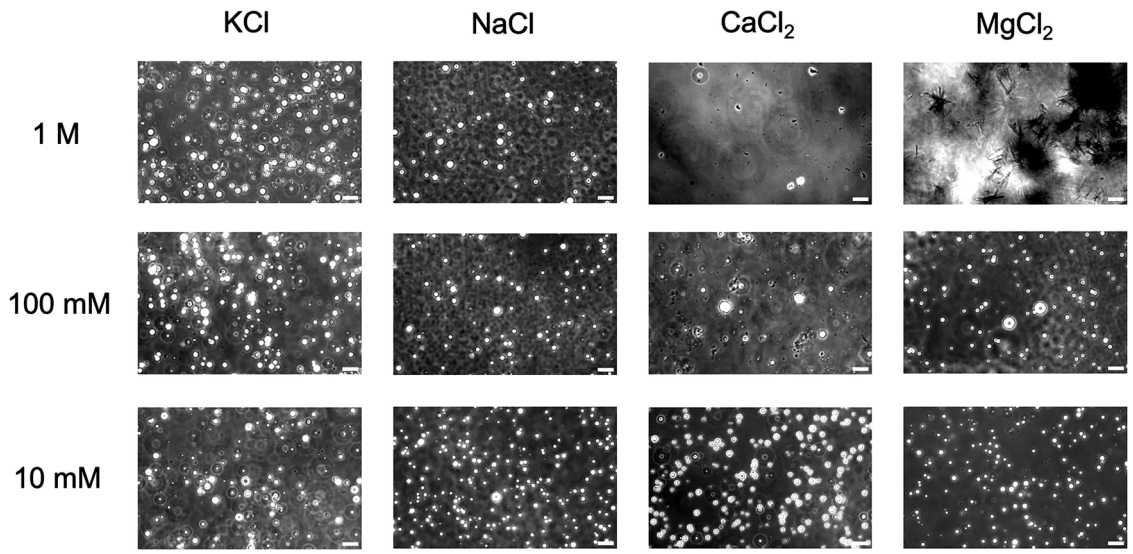

Fig. 5 Representative microscopy images of polyLA samples polymerized in various salts at varying concentrations, with a constant 500 µL reaction volume. Scale bars: 50 µm. Additional microscopy images are available in Supplementary Figs. S2–S5

the presence of salts, but salts can alter the surface tension and destabilize MMDs by neutralizing the negatively charged droplet surfaces [16], which led to MMD coalescence. To characterize the influence of salts on the synthesis of LA-containing polymers, we subjected LA (final 250 mM concentration) to NaCl, KCl, $MgCl_2$, or $CaCl_2$, each at 1 M, 100 mM, and 10 mM, to dehydration synthesis for 5–6 days at 80 °C, followed by MALDI-ToF-MS analysis. Based on our findings in this study, LA polymerization could still occur in the presence of all salts at 10 mM (Fig. 3A). At concentrations of 100 mM, NaCl, KCl, and $MgCl_2$ allowed the polymerization process to occur, but $CaCl_2$ appeared to hinder the polymerization process (Fig. 3B). At 1 M (Fig. 3C), NaCl and KCl still allowed LA polymerization, but both $MgCl_2$ and $CaCl_2$ hindered the polymerization process. Peaklists of spectra in Fig. 3 with evidence of polyLA formation are presented in Supplementary Tables S1–S9. Comparable results were observed in the spectra obtained from MALDI-ToF-MS using the DCTB matrix, as shown in Supplementary Fig. S1 and Supplementary Tables S10–S18. Next, semi-quantitative analysis by estimating the center of mass and the length of the polyLA products (*Materials and Methods*) (Fig. 4 and Supplementary Table S19) confirms these observations and suggests that higher concentrations of divalent salts inhibit LA polymerization while increasing monovalent salt concentration does not appear to affect polymerization. Additionally, among the divalent ions, Ca^{2+} appears to hinder polymerization to a greater degree than Mg^{2+}. A possible mechanism for this inhibitory effect is the stronger interaction of divalent cations with the -COOH group of LA, leading to the potential formation of stable metal-lactate complexes, unlike with monovalent cations [60]. This reduces the availability of free, protonated LA monomers necessary for ester bond formation during dehydration polymerization. This pattern of influence of these salts on LA polymerization is similar to the influence of the same salts on PA polymerization [16, 37], with divalent salts exhibiting more inhibitory character than monovalent salts. Similarly, Ca^{2+} was shown to bind more strongly to -COOH than Mg^{2+}, which appears to agree with our results where Mg^{2+} inhibits LA polymerization at 1 M, while Ca^{2+} exhibits inhibitory effects at 100 mM. A similar trend was observed in primitive depsipeptide polymerization reactions, with Ca^{2+} showing a greater inhibitory effect than Mg^{2+} [61].

Next, to assess the ability of salts at various concentrations to affect the ability of the polyLA products to assemble into MMDs, we performed microscopy analysis on the polyLA gel products after rehydration in 4:1/water:acetonitrile (Fig. 5, Supplementary Figs. S2–S5). The microscopy images reveal that phase transition and formation of MMDs of polyLA synthesized in the presence of KCl and NaCl occurred at all salt concentrations. However, it is noticeable that droplet assembly could be consistently observed only in samples synthesized at lower concentrations of the divalent salts $CaCl_2$ (10 mM) and $MgCl_2$ (10 and 100 mM); these observations match roughly with the polymerization results and suggest that only reactions with polymerized polyLA products could assemble into microdroplets. For $CaCl_2$ specifically, microscopy analyses did reveal some images that may have indicated possible MMD assembly at 100 mM $CaCl_2$ but were not consistently observed in all trials, suggesting that consistent droplet assembly is possible only at lower $CaCl_2$ concentrations. After cross-confirming the MALDI-ToF-MS data, which showed that polyLA could not be detected in the presence of 100 mM $CaCl_2$, we speculate that some of the structures observed could also have been aggregates. It is also

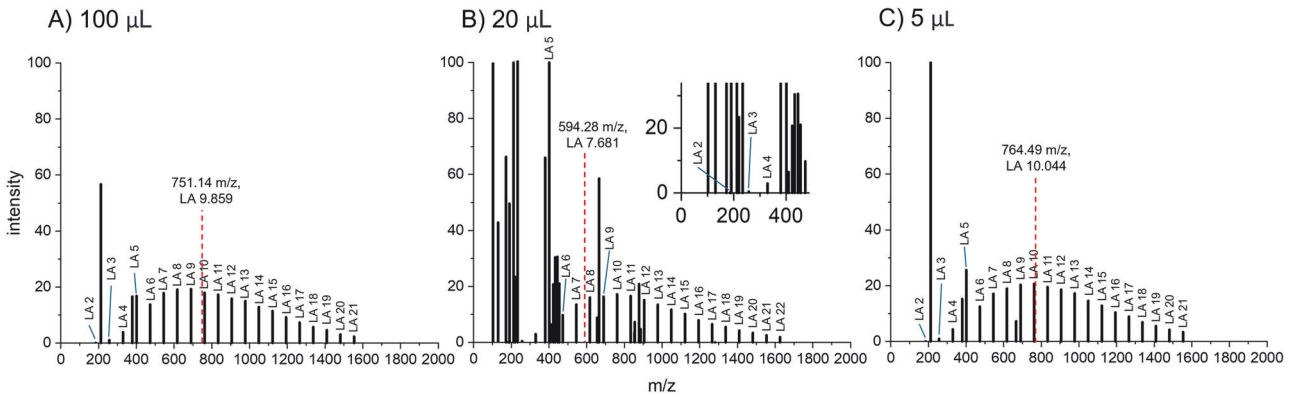

Fig. 6 Comparison of MALDI-ToF-MS spectra (CHCA matrix) of LA products synthesized from variable initial reaction volumes of **A** 100 µL, **B** 20 µL, and **C** 5 µL at a constant 500 mM reactant concentration. Labeled peaks are sodiated ($M+Na^+$). The estimated center of mass (m/z) and length (mers) of LA products measured for each spectrum are denoted by thin red dashed lines. Peaklists of these spectra with evidence of polyLA formation are presented in Supplementary Tables S20–S22. Similar results were observed in MALDI-ToF-MS spectra using DCTB as the matrix, which are presented in Supplementary Fig. S6 along with their peak lists in Supplementary Tables S23–S25

possible that some LA polymerization did occur to some degree in the presence of 100 mM $CaCl_2$ but could not be detected by MALDI-ToF-MS due to instrument sensitivity reasons or ion suppression.

These findings have implications for understanding the environmental conditions conducive to LA polymerization and MMD formation on early Earth. High concentrations of monovalent salts, such as NaCl and KCl, which are typically associated with evaporative coastal environments [62], which could lead to smaller water bodies such as small pores or pools, or hypersaline brine pools [63–65] could have supported robust LA polymerization and MMD assembly on early Earth. Conversely, intermediate or high concentrations of divalent salts, such as $CaCl_2$ and $MgCl_2$, common in mineral-rich springs or carbonate-dominated regions, would have likely hindered primitive LA polymerization and MMD assembly [66]. Such high concentrations of divalent salt environments may have limited the prevalence of polyLA microdroplets, suggesting that the local ionic composition would have been a critical factor in the emergence and stability of prebiotic compartments. For example, places on modern Earth such as the Hephaestus brine, Kryos brine, and Discovery brine in the Mediterranean Sea [67] contain high concentrations of Na^+, K^+, Mg^{2+}, Ca^{2+}, and Cl^-; Don Juan Pond, Antarctica [68, 69] possibly contains high concentrations of $CaCl_2$ and NaCl, and the Atacama Desert, Chile possibly contains high concentrations of NaCl, which could serve as analogs for LA polymerization processes leading to MMD formation. These observations suggest that similar saline aqueous media may have existed on early Earth. Additionally, extraterrestrial aqueous environments [49, 70–75] may also have variable salinities. For instance, saline environments of Mg^{2+} and Na^+ salts were reported to possibly exist on the Martian surface [76], whereas Ganymede [77, 78], Europa [79], and Enceladus [80] may harbor environments with both monovalent and divalent salts of Na^+, Mg^{2+}, and Ca^{2+} ions. If LA were to be present in these environments, our study provides valuable insights into the potential for polyester and MMD formation under these extraterrestrial conditions. Similarly, it is plausible for polyLA droplets to form first in low-salt environments and then be transported to other locales with higher salinity. Previous studies suggested that significant salt introduction to polyPA microdroplets resulted in increased coalescence due to neutralization of the negative droplet surface charge; divalent salts exhibited a stronger neutralization effect than monovalent salts [16]. We speculate that a similar trend may also be observed in polyLA as well. Collectively, our findings shed light on salt conditions amenable to LA polymerization and MMD assembly and help to frame the plausible existence of polyester MMDs on early Earth, highlighting how salt composition could play a pivotal role in such polymerization processes.

Lower reaction volume and reactant concentration influence the synthesis of LA polymers

Next, we explored the polymerization of LA monomers under dehydration conditions across variable initial reaction volumes and reactant concentrations. We first subjected LA stock solutions (500 mM) to dehydration at 80 °C in low volumes of 100 µL, 20 µL, and 5 µL over 5–6 days until complete dryness (Fig. 2). The resulting gel-like substances were analyzed *via* MALDI-ToF-MS, revealing the formation of polyLA with lengths up to the range of ~21-mers across all reaction volumes (Fig. 6 and Supplementary Fig. S6, Supplementary Tables S20–S25). Specifically, the center of polymer mass and average polymer length of each variable volume reaction, estimated semi-quantitatively, did

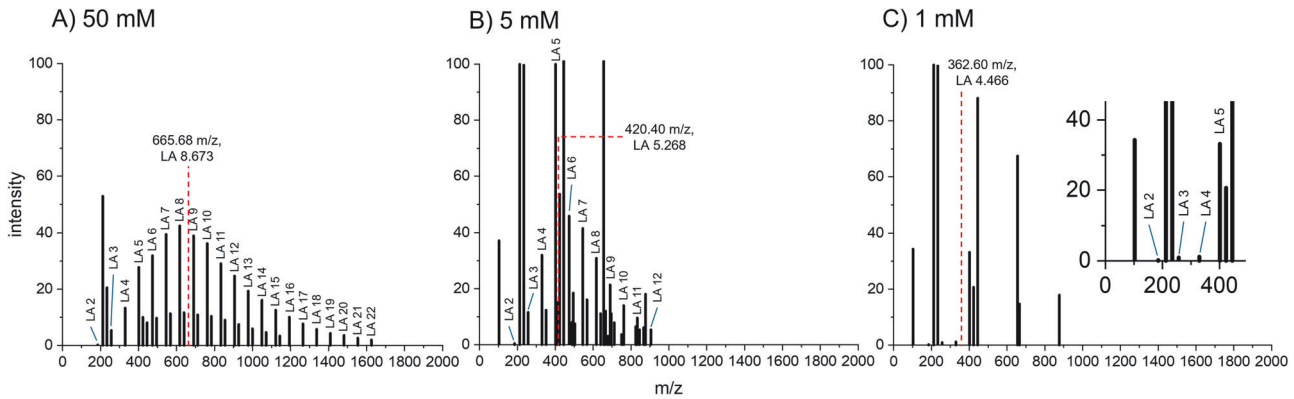

Fig. 7 Comparison of MALDI-ToF-MS spectra (CHCA matrix) of LA synthesis under varying LA reactant concentrations of **A** 50 mM, **B** 5 mM, and **C** 1 mM at a constant 500 µL reaction volume. Labeled peaks are sodiated ($M+Na^+$). The estimated center of mass (m/z) and length (mers) of LA products measured for each spectrum are denoted by thin red dashed lines. Peaklists of these spectra with evidence of polyLA formation are presented in Supplementary Tables S26–S28. Similar results were observed in MALDI-ToF-MS spectra using DCTB as the matrix, which are presented in Supplementary Fig. S7 along with their peak lists in Supplementary Tables S29–S31

not significantly differ across reaction volumes, indicating that polymerization appeared to occur efficiently even at significantly reduced volumes (Fig. 6).

Similarly, when the LA reactant concentration was varied at a constant reaction volume of 500 µL (50 mM, 5 mM, and 1 mM), MALDI-ToF-MS analysis of the reaction products revealed that the LA polymer product length appeared to be somewhat dependent on the reactant concentration (Figs. 7 and Supplementary Fig. S7, Supplementary Tables S26–S31). At 50 mM, the polymer lengths reached up to 22-mers, while reactions at 5 mM and 1 mM yielded shorter polymers with length maxima of 12-mers and 5-mers, respectively. We next calculated the estimated center of polymer mass and length (Fig. 7) of each variable concentration reaction, and our semi-quantitative calculation revealed that the center of the LA polymer mass appears to shift towards lower m/z values as the concentration decreases, indicating a likely reduction in the average polymer length at lower reaction concentrations. This phenomenon opens up a possibility that a lower concentration could result in further reduction or complete inhibition of LA polymerization, and we speculate that reactions containing micromolar-range concentrations of LA could result in no product formation. Having said that, the synthesis of polyLA under both varying volumes and concentrations exhibit a pattern similar to our previous observations in polymerization studies using PA as the starting material under comparable conditions [37], suggesting that perhaps our observations for both LA and PA could be generalized to other AHAs as well.

However, we also speculate that LA evaporation (due to its boiling point of 122 °C) may result in loss of LA, which could contribute to product formation inhibition especially in high-volume (500 µL) cases (such as in Fig. 7), due to the requirement of a longer reaction (i.e., evaporation) time to achieve full dryness. Weight-based measurements (*Materials and Methods*) suggest that more than 50% of the initial LA is likely lost to accumulative evaporation over the reaction period (~one week) for 500 µL reactions. Although for high volume, high concentration (i.e., 50 mM) cases, a significant proportion of the initial LA reactant is lost to evaporation over the reaction period, the initial concentration of LA is sufficiently high, which allows a high enough solution concentration to remain and produce a significant amount of polymer products. On the other hand, in high-volume, low-concentration cases (i.e., 1 mM), as the initial LA concentration is not high, LA lost to evaporation will significantly affect the ability for polymer products to be produced. This phenomenon was not as apparent for phenyllactic acid (PA polymerization), where we observed polymerization even at 1 mM [37]. This is likely due to the fact that PA has a much higher boiling point (363 °C) compared to LA. However, the system studied herein also contains (1) LA monomers, which may form H-bonds with each other and water; (2) cyclic LA dimers, which could form from dimerization of LA monomers and increase the boiling point; and (3) LA oligomers, where each oligomeric addition increases the boiling point of the oligomer. Thus, these three effects suggest that our system may not be a simple, non-interacting liquid, which suggests that LA evaporative loss could actually be minimized compared to any calculated "theoretical" amount. Nevertheless, to fully understand the evaporative process, more detailed modeling is required, which is beyond the scope of this study.

Subsequently, to assess the ability of polyLA samples synthesized under both varying reaction volumes and reactant concentrations to form MMDs, we performed microscopy imaging analysis on each polymerization product after rehydration in 4:1 water:acetonitrile. Microscopy images revealed robust MMD assembly in the 100 µL reactions, whereas the 20 µL and 5 µL reactions displayed fewer and less distinct droplet-like structures (Fig. 8 and

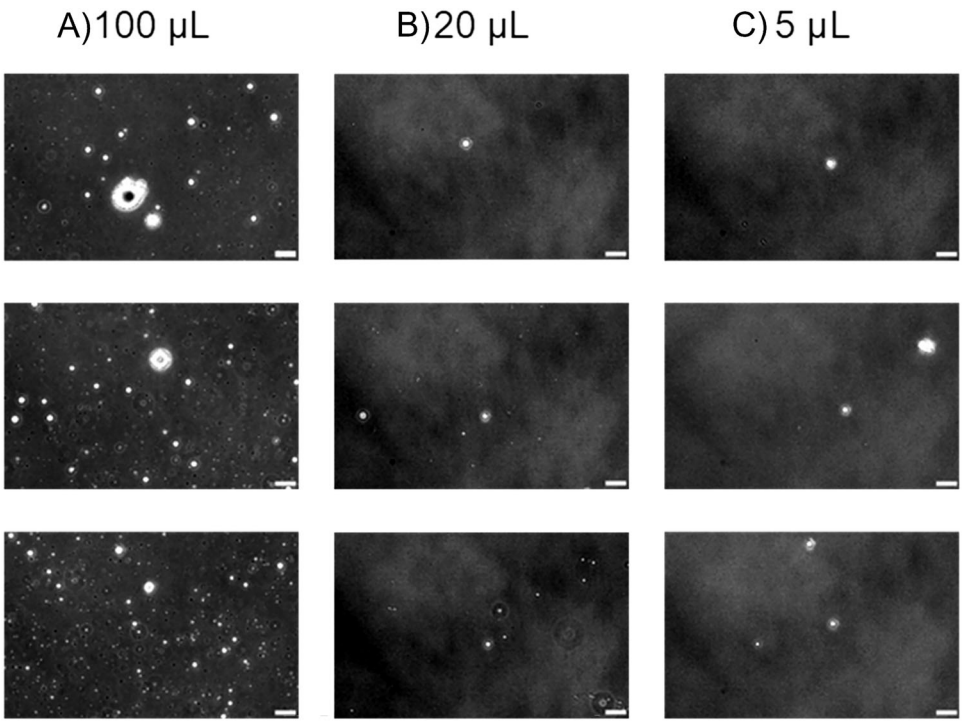

Fig. 8 Representative microscopy images of LA products synthesized from variable reaction volumes of **A** 100 µL, **B** 20 µL, and **C** 5 µL in polymerization reactions at a constant 500 mM reactant concentration. Three different images of each sample are shown to demonstrate the reproducibility. Scale bars: 20 µm

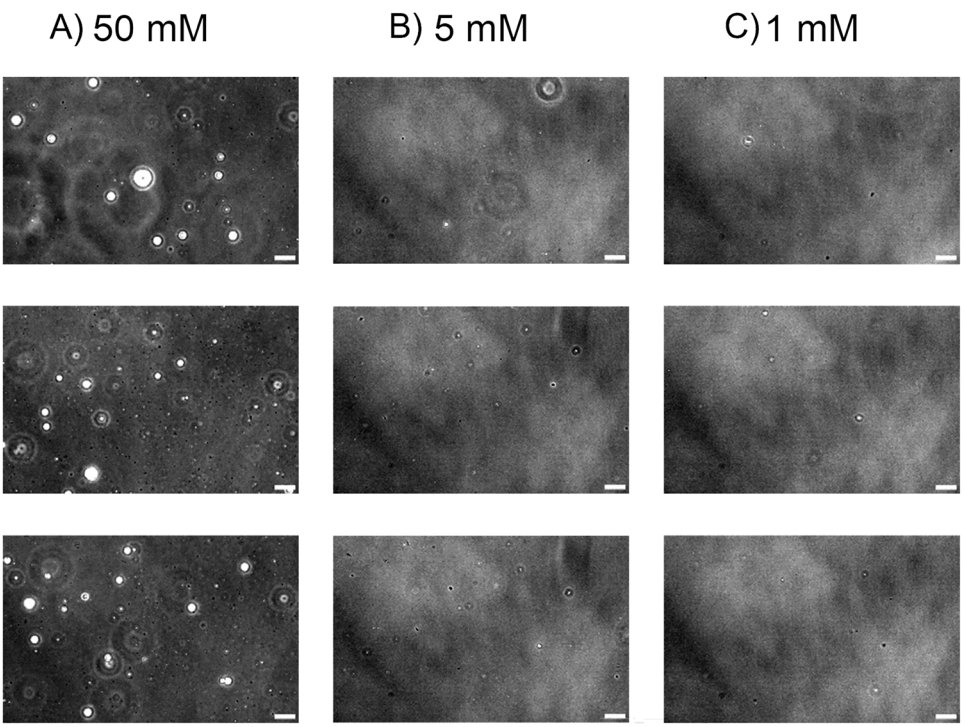

Fig. 9 Representative microscopy images of LA products synthesized from variable reactant concentrations of **A** 50 mM, **B** 5 mM, and **C** 1 mM in polymerization reactions at a constant 500 µL reaction volume. Three different images of each sample are shown to demonstrate the reproducibility. Scale bars: 20 µm

Supplementary Fig. S8). Referring to MALDI-ToF-MS data, which revealed the occurrence of LA polymerization in 20 µL and 5 µL reaction volumes, we speculate that the sparse droplet-like structures seen in rehydrated LA 20 µL and 5 µL product samples are indeed likely MMDs and that the lower density of MMDs observed in lower reaction volume samples could be due to the lower yield of polymers formed from a lower gross amount of LA starting material used. Similarly, polymerization products produced with variable reactant concentrations showed similar trends as those observed in reactions with varying reaction volumes in the context of MMD assembly (Fig. 9 and Supplementary Fig. S9). Specifically, microscopy images revealed robust MMD assembly for polyLA samples synthesized at LA

concentrations of 50 mM. However, for the LA samples synthesized at concentrations of 5 mM and 1 mM, the droplets, while present to some extent, are not as readily observable and are less dense compared to the 50 mM-LA samples, which appears to be in rough agreement with MALDI-ToF-MS analyses indicating shorter products and apparently lower yields for reactions at lower concentrations. Lower polyLA product yields (due to less gross starting material) thus result in lower MMD assembly propensity. Similarly, shorter product polyLA lengths could also lead to lower MMD assembly propensity, as the proposed mechanism for MMD assembly relies on hydrophobic interactions among product polymers, which become less apolar with decreasing product length.

These results combined suggest that polyLA can form MMDs even as products of reactions where LA concentrations and volumes are much lower than 500 mM and 500 µL, respectively, and potentially down to the sub-mM/µL range, suggesting a wider plausibility of polyLA existence on early Earth. These results underscore the important role of both initial reaction volume and reactant concentration in driving primitive LA polymerization and MMD assembly. The interplay between reaction volume and LA reactant concentration could highlight a delicate balance in terms of volume and concentration. While reduced reaction volume appears to not inhibit polymerization, gross polymer yield could be reduced, which potentially reduces MMD density upon rehydration. However, such polymerization and MMD assembly could still be possible in primitive aqueous microenvironments such as rock pores [81], atmospheric aerosols [82], or even sea spray [83], which possibly existed at the scale of a few microlitres. Conversely, lower LA monomer reactant concentrations appear to not only reduce polymer yield but also lead to shorter polymer product lengths. This suggests that perhaps primitive scenarios conducive to polyLA polymerization would require sufficient concentrations of LA monomers to enable polymerization and subsequent MMD assembly.

Conclusion

The findings of this study demonstrate the critical influence of the environmental conditions and locations on early Earth, such as salt types, reaction volumes, and reactant concentrations, on the polymerization and assembly of LA-containing polyester polymers, shedding light on the potential mechanisms that could have driven the polymerization and assembly of early biopolymers, which are likely critical steps in the emergence of life on prebiotic Earth. Our study revealed that monovalent salts such as NaCl and KCl do not inhibit LA polymerization and MMD assembly even up to high concentrations such as 1 M, whereas divalent salts such as $MgCl_2$ and $CaCl_2$ were found to hinder the polymerization process at higher concentrations. Thus, certain salts could have allowed polyester polymerization processes under prebiotic conditions, while others could have posed constraints. Moreover, this study highlights that lower reaction volumes and concentrations, which may mimic confined microenvironments on early Earth, may still allow LA polymerization and MMD assembly, but these conditions could result in less robust LA polymerization and MMD assembly, possibly due to the decreased product yield of polyLA. Despite these limitations, MMD assembly from polyLA samples was observed even at initial LA concentrations as low as 1 mM and volumes as low as 5 µL, suggesting that lower concentrations and volumes can still support MMD assembly, albeit with reduced efficiency. These observations align with previous studies on PA polymers [16, 37], suggesting that our observations could be extended to be generally applicable to other AHAs, although more specific studies may be needed. This study underscores the importance of variations in ionic compositions and salt identities, environmental confinement, and reactant concentrations in understanding the mechanisms that may have driven the transition from simple molecules to complex, life-like systems, offering valuable insights into the origins of life. Future work should explore the effects of other environmental variables and diverse AHA monomers that can form polyesters and promote subsequent MMD formation to further elucidate potential pathways for the assembly of the first compartments on Earth.

Acknowledgements MS, NT, and KC are supported by the Ministry of Higher Education Malaysia (MoHE) through the Fundamental Research Grant Scheme under the grant number FRGS/1/2021/STG04/UKM/02/1 and the Visitor Grant (ZF-2022-008). CC is supported by a RIKEN Special Postdoctoral Researchers (SPDR) fellowship and JSPS Grants-in-Aid for Early Career Scientists 24K17795. P-HW is supported by the National Science and Technology Council of Taiwan (111-2628-E-008-009). TZJ is supported by JSPS Grants-in-aid 18K14354 and 21K14746, a Tokyo Institute of Technology Yoshinori Ohsumi Fund for Fundamental Research, the Mizuho Foundation for the Promotion of Science, and the Temporary Assistant Program by the DE&I Section of Science Tokyo (formerly Tokyo Institute of Technology) (facilitated by K Fujishima, whom TZJ acknowledges). KC is also supported by the Alexander von Humboldt Foundation. Funds for MS to visit ELSI for collaborative work on this project were partially supported by a travel grant by the ELSI Director's Office Visitor Program (Brain Exchange) to TZJ; the same program also funded a visit to ELSI by M-JH for her master's thesis project (however, the program did not fund the visit of NT to ELSI, which was funded by other means due to a change in the terms of the Brain Exchange program in fiscal year 2024; from fiscal year 2025, student visits are categorically no longer funded by this program). Funds for ND to visit ELSI for collaborative work on this project were provided in-part by a scholarship from the China Scholarship Council. The authors thank M. Koizumi (Institute of Science, Tokyo (formerly Tokyo Institute of Technology) Materials Analysis Division) for assistance with MALDI-ToF-MS analysis.

Author contributions RA, TZJ, and KC conceptualized the project. M-JH, CC, RY, P-HW, TZJ, and KC designed experiments. MS, M-JH, and RA performed experiments. MS, M-JH, NT, RA, ND, P-HW, TZJ, and KC analyzed data. MS, NT, TZJ, and KC wrote the first draft of the manuscript, and all authors contributed to the editing of the final draft.

Compliance with ethical standards

Conflict of interest The authors declare no competing interests.

Publisher's note Springer Nature remains neutral with regard to jurisdictional claims in published maps and institutional affiliations.

Open Access This article is licensed under a Creative Commons Attribution 4.0 International License, which permits use, sharing, adaptation, distribution and reproduction in any medium or format, as long as you give appropriate credit to the original author(s) and the source, provide a link to the Creative Commons licence, and indicate if changes were made. The images or other third party material in this article are included in the article's Creative Commons licence, unless indicated otherwise in a credit line to the material. If material is not included in the article's Creative Commons licence and your intended use is not permitted by statutory regulation or exceeds the permitted use, you will need to obtain permission directly from the copyright holder. To view a copy of this licence, visit http://creativecommons.org/licenses/by/4.0/.

References

1. Chandru K, Potiszil C, Jia TZ. Alternative pathways in astrobiology: Reviewing and synthesizing contingency and non-biomolecular origins of terrestrial and extraterrestrial life. Life. 2024;14:1069.
2. Poddar A, Satthiyasilan N, Wang P-H, Chen C, Yi R, Chandru K, et al. Reactions Driven by Primitive Nonbiological Polyesters. Acc Chem Res. 2024;57:2048–57.
3. Chandru K, Mamajanov I, Cleaves HJ II, Jia TZ. Polyesters as a model system for building primitive biologies from non-biological prebiotic chemistry. Life. 2020;10:6.
4. Nelsestuen GL. Origin of life: consideration of alternatives to proteins and nucleic acids. J Mol Evol. 1980;15:59–72.
5. Miller SL. Production of Some Organic Compounds under Possible Primitive Earth Conditions1. J Am Chem Soc. 1955;77:2351–61.
6. Parker ET, Cleaves HJ II, Bada JL, Fernández FM. Quantitation of α-hydroxy acids in complex prebiotic mixtures via liquid chromatography/tandem mass spectrometry. Rapid Commun Mass Spectrom. 2016;30:2043–51.
7. Zang X, Ueno Y, Kitadai N. Photochemical synthesis of ammonia and amino acids from nitrous oxide. Astrobiology. 2022;22:387–98.
8. Barge LM, Flores E, Baum MM, VanderVelde DG, Russell MJ. Redox and pH gradients drive amino acid synthesis in iron oxyhydroxide mineral systems. Proc Natl Acad Sci USA. 2019;116:4828–33.
9. Peltzer ET, Bada JL, Schlesinger G, Miller SL. The chemical conditions on the parent body of the Murchison meteorite: some conclusions based on amino, hydroxy and dicarboxylic acids. Adv Space Res. 1984;4:69–74.
10. Li Y, Kurokawa H, Sekine Y, Kebukawa Y, Nakano Y, Kitadai N, et al. Aqueous breakdown of aspartate and glutamate to n-ω-amino acids on the parent bodies of carbonaceous chondrites and asteroid Ryugu. Sci Adv. 2023;9:eadh7845.
11. Ross DS, Deamer D. Dry/Wet Cycling and the Thermodynamics and Kinetics of Prebiotic Polymer Synthesis. Life. 2016;6:28.
12. Chandru K, Guttenberg N, Giri C, Hongo Y, Butch C, Mamajanov I, et al. Simple prebiotic synthesis of high diversity dynamic combinatorial polyester libraries. Commun Chem. 2018;1:30.
13. Jia TZ, Chandru K. Recent progress in primitive polyester synthesis and membraneless microdroplet assembly. Biophys Physicobiol. 2023;20:e200012.
14. Forsythe JG, Yu S-S, Mamajanov I, Grover MA, Krishnamurthy R, Fernández FM, et al. Ester-mediated amide bond formation driven by wet-dry cycles: A possible path to polypeptides on the prebiotic Earth. Angew Chem Int Ed Engl. 2015;54:9871–5.
15. Jia TZ, Chandru K, Hongo Y, Afrin R, Usui T, Myojo K, et al. Membraneless polyester microdroplets as primordial compartments at the origins of life. Proc Natl Acad Sci USA. 2019;116:15830–5.
16. Chen C, Yi R, Igisu M, Sakaguchi C, Afrin R, Potiszil C, et al. Spectroscopic and biophysical methods to determine differential salt-uptake by primitive membraneless polyester microdroplets. Small Methods. 2023;7:e2300119.
17. Jia TZ, Bapat NV, Verma A, Mamajanov I, Cleaves HJ II, Chandru K. Incorporation of Basic α-Hydroxy Acid Residues into Primitive Polyester Microdroplets for RNA Segregation. Biomacromolecules. 2021;22:1484–93.
18. dos Santos EC, Angelini A, Hürlimann D, Meier W, Palivan CG. Giant polymer compartments for confined reactions. Chemistry. 2020;2:470–89.
19. Shum HC, Zhao Y-J, Kim S-H, Weitz DA. Multicompartment Polymersomes from Double Emulsions. Angew Chem Int Ed Engl. 2011;50:1648–51.
20. Cleaves HJ II. Prebiotic chemistry: What we know, what we don't. Evolution. 2012;5:342–60.
21. Knauth LP. Salinity history of the Earth's early ocean [letter]. Nature. 1998;395:554–5.
22. Knauth LP. Temperature and salinity history of the Precambrian ocean: implications for the course of microbial evolution. Palaeogeogr Palaeoclimatol Palaeoecol. 2005;219:53–69.
23. Albarede F, Thibon F, Blichert-Toft J, Tsikos H. Chemical archeoceanography. Chem Geol. 2020;548:119625.
24. Olson S, Jansen MF, Abbot DS, Halevy I, Goldblatt C. The effect of ocean salinity on climate and its implications for Earth's habitability. Geophys Res Lett. 2022;49:e2021GL095748.
25. Steller LH, Van Kranendonk MJ, Wang A. Dehydration enhances prebiotic lipid remodeling and vesicle formation in acidic environments. ACS Cent Sci. 2022;8:132–9.
26. Maheen G, Wang Y, Wang Y, Shi Z, Tian G, Feng S. Mimicking the prebiotic acidic hydrothermal environment: One-pot prebiotic hydrothermal synthesis of glucose phosphates. Heteroat Chem. 2011;22:186–91.
27. Bassez M-P. Is high-pressure water the cradle of life?. J Phys Condens Matter. 2003;15:L353–61.
28. Kapoor S, Berghaus M, Suladze S, Prumbaum D, Grobelny S, Degen P, et al. Prebiotic cell membranes that survive extreme environmental pressure conditions. Angew Chem Int Ed Engl. 2014;53:8397–401.
29. Todd ZR, Lozano GG, Kufner CL, Ranjan S, Catling DC, Sasselov DD. UV transmission in prebiotic environments on early earth. Astrobiology. 2024;24:559–69.
30. Brennan ST, Lowenstein TK, Cendon DI. The major-ion composition of Cenozoic seawater: The past 36 million years from fluid inclusions in marine halite. Am J Sci. 2013;313:713–75.
31. Sahai N, Adebayo S, Schoonen MA. Freshwater and evaporite brine compositions on Hadean earth: Priming the origins of life. Astrobiology. 2022;22:641–71.
32. Cohen NR, Noble AE, Moran DM, McIlvin MR, Goepfert TJ, Hawco NJ, et al. Hydrothermal trace metal release and microbial

metabolism in the northeastern Lau Basin of the South Pacific Ocean. Biogeosciences. 2021;18:5397–422.
33. Shinohara H, Geshi N, Yokoo A, Ohkura T, Terada A. Salt shell fallout during the ash eruption at the Nakadake crater, Aso volcano, Japan: evidence of an underground hydrothermal system surrounding the erupting vent. Earth Planets Space. 2018;70:46.
34. Nielsen SG, Klein F, Marschall HR, Pogge von Strandmann PAE, Auro M. Magnesium isotope fractionation processes during seafloor serpentinization and implications for serpentinite subduction. Solid Earth. 2024;15:1143–54.
35. Jerabek-Willemsen M, Wienken CJ, Braun D, Baaske P, Duhr S. Molecular interaction studies using microscale thermophoresis. Assay Drug Dev Technol. 2011;9:342–53.
36. Marien YW, Van Steenberge PHM, R. D'hooge D, Marin GB. Particle by particle kinetic Monte Carlo tracking of reaction and mass transfer events in miniemulsion free radical polymerization. Macromolecules. 2019;52:1408–23.
37. Sithamparam M, Afrin R, Tharumen N, He M-J, Chen C, Yi R, et al. Probing the limits of reactant concentration and volume in primitive polyphenyllactate synthesis and microdroplet assembly processes. ACS Bio Med Chem Au. 2025;5:131–42.
38. Kahana A, Schmitt-Kopplin P, Lancet D. Enceladus: First observed primordial soup could arbitrate origin-of-life debate. Astrobiology. 2019;19:1263–78.
39. Sephton MA. Organic matter in ancient meteorites. Astron Geophys. 2004;45:2.08–14.
40. Chandru K, Jia TZ, Mamajanov I, Bapat N, Cleaves HJ II. Prebiotic oligomerization and self-assembly of structurally diverse xenobiological monomers. Sci Rep. 2020;10:17560.
41. Afrin R, Chen C, Sarpa D, Sithamparam M, Yi R, Giri C, et al. The effects of dehydration temperature and monomer chirality on primitive polyester synthesis and microdroplet assembly. Macromol Chem Phys. 2022;223:2200235.
42. Takano Y, Naraoka H, Dworkin JP, Koga T, Sasaki K, Sato H, et al. Primordial aqueous alteration recorded in water-soluble organic molecules from the carbonaceous asteroid (162173) Ryugu. Nat Commun. 2024;15:5708.
43. Aponte JC, Elsila JE, Hein JE, Dworkin JP, Glavin DP, McLain HL, et al. Analysis of amino acids, hydroxy acids, and amines in CR chondrites. Meteorit Planet Sci. 2020;55:2422–39.
44. Taran O, Unal B. Anoxic photolysis as a route to primary metabolites on early Earth. ChemRxiv. 2024, https://doi.org/10.26434/chemrxiv-2024-w7svp.
45. Deal AM, Vaida V. Oxygen effect on the ultraviolet-C photochemistry of lactic acid. J Phys Chem A. 2023;127:2936–45.
46. Mulkidjanian AY, Bychkov AY, Dibrova DV, Galperin MY, Koonin EV. Origin of first cells at terrestrial, anoxic geothermal fields. Proc Natl Acad Sci USA. 2012;109:E821–30.
47. Maurer SE, Tølbøl Sørensen K, Iqbal Z, Nicholas J, Quirion K, Gioia M, et al. Vesicle self-assembly of monoalkyl amphiphiles under the effects of high ionic strength, extreme pH, and high temperature environments. Langmuir. 2018;34:15560–8.
48. Fernanders MS, Gough RV, Chevrier VF, Schiffman ZR, Ushijima SB, Martinez GM, et al. Water uptake by chlorate salts under Mars-relevant conditions. Icarus. 2022;371:114715.
49. Napoleoni M, Klenner F, Khawaja N, Hillier JK, Postberg F. Mass spectrometric fingerprints of organic compounds in NaCl-rich ice grains from Europa and Enceladus. ACS Earth Space Chem. 2023;7:735–52.
50. Travis BJ, Palguta J, Schubert G. A whole-moon thermal history model of Europa: Impact of hydrothermal circulation and salt transport. Icarus. 2012;218:1006–19.
51. Villafañe-Barajas SA, Baú JPT, Colín-García M, Negrón-Mendoza A, Heredia-Barbero A, Pi-Puig T, et al. Salinity effects on the adsorption of nucleic acid compounds on Na-montmorillonite: A prebiotic chemistry experiment. Orig Life Evol Biosph. 2018;48:181–200.
52. Joshi PC, Aldersley MF. Significance of mineral salts in prebiotic RNA synthesis catalyzed by montmorillonite. J Mol Evol. 2013;76:371–9.
53. Maurer SE, Nguyen G. Prebiotic vesicle formation and the necessity of salts. Orig Life Evol Biosph. 2016;46:215–22.
54. Morth JP, Pedersen BP, Buch-Pedersen MJ, Andersen JP, Vilsen B, Palmgren MG, et al. A structural overview of the plasma membrane Na+,K+-ATPase and H+-ATPase ion pumps. Nat Rev Mol Cell Biol. 2011;12:60–70.
55. Stanley KS, Young VC, Gatto C, Artigas P. External ion access in the Na/K pump: Kinetics of Na+, K+, and Quaternary Amine interaction. Biophys J. 2018;115:361–74.
56. Yang Z, Hayes JJ. The divalent cations Ca2+ and Mg2+ play specific roles in stabilizing histone-DNA interactions within nucleosomes that are partially redundant with the core histone tail domains. Biochemistry. 2011;50:9973–81.
57. Williams RJP. The evolution of the biochemistry of calcium. In: Krebs J, Michalak M. editors, Calcium - A Matter of Life or Death. Elsevier, Amsterdam; Netherlands; 2007. pp. 23–48.
58. Erulkar SD. The versatile role of calcium in biological systems. Interdiscip Sci Rev. 1981;6:322–32.
59. Lin Y-C, Broedersz CP, Rowat AC, Wedig T, Herrmann H, MacKintosh FC, et al. Divalent cations crosslink vimentin intermediate filament tail domains to regulate network mechanics. J Mol Biol. 2010;399:637–44.
60. Kherb J, Flores SC, Cremer PS. Role of Carboxylate Side Chains in the Cation Hofmeister Series. J. Phys. Chem. B. 2012;116:7389–97.
61. Frenkel-Pinter M, Sargon AB, Glass JB, Hud NV, Williams LD. Transition metals enhance prebiotic depsipeptide oligomerization reactions involving histidine. RSC Adv. 2021;11:3534–8.
62. Ding T, Liu C, Guo F, Zhao Y, Wang M, Chen L. 2020. Evaporation Stage of Paleo-saline Lake in the Sichuan Basin, China: Insight from Fluid inclusions in Halite. Acta Geol Sin. 2020;94:801–8.
63. Oren A. Life in magnesium- and calcium-rich hypersaline environments: Salt stress by chaotropic ions. In: Seckbach J, Oren A, Stan-Lotter, H, editors Polyextremophiles. Cellular Origin, Life in Extreme Habitats and Astrobiology. Springer; Dordrecht; Netherlands; 2013. pp. 215–32.
64. Zhang B, Yang K, Wang X, Xu Z, Yang H, Zhang S, et al. Salt-gathering and potassium formation of potassium-rich brine during the Triassic in the Sichuan Basin, China. Acta Geol Sin. 2018;92:2233–50.
65. Ding T, Liu C, Zhao Y, Zhu Z. Chlorine isotope analysis of Triassic salt rock and geological significance of ancient salt lake in Sichuan Basin, China. Carbonates Evaporites. 2019;34:909–15.
66. Dalai P, Ustriyana P, Sahai N. Aqueous magnesium as an environmental selection pressure in the evolution of phospholipid membranes on early earth. Geochim Cosmochim Acta. 2018;223:216–28.
67. La Cono V, Bortoluzzi G, Messina E, La Spada G, Smedile F, Giuliano L, et al. The discovery of Lake Hephaestus, the youngest athalassohaline deep-sea formation on Earth. Sci Rep. 2019;9:1679.
68. Dickson JL, Head JW, Levy JS, Marchant DR. Don Juan Pond, Antarctica: near-surface CaCl(2)-brine feeding Earth's most saline lake and implications for Mars. Sci Rep. 2013;3:1166.
69. Marion GM. A theoretical evaluation of mineral stability in Don Juan Pond, Wright Valley, Victoria Land. Antarct Sci. 1997;9:92–99.
70. German C, Institution WHO, Arrigo K, Murray A, Rhoden A. Planetary oceanography: Leveraging expertise among Earth and planetary science. Oceanography. 2022;35:10–15.

71. Matsumoto T, Noguchi T, Miyake A, Igami Y, Matsumoto M, Yada T, et al. Sodium carbonates on Ryugu as evidence of highly saline water in the outer Solar System. Nat Astron. 2024;8:1536–43.
72. Bhardwaj A, Sam L, Martín-Torres F, Zorzano M-P, Ramírez Luque J. UAV imaging of a Martian brine analogue environment in a fluvio-aeolian setting. Remote Sens. 2019;11:2104.
73. Barbieri R, Stivaletta N. Continental evaporites and the search for evidence of life on Mars: ASTROBIOLOGY OF CONTINENTAL EVAPORITES. Geol J. 2011;46:513–24.
74. Osterloo MM, Scott Anderson F, Hamilton VE, Hynek BM. Geologic context of proposed chloride-bearing materials on Mars. J Geophys Res Planets. 2010;115, https://doi.org/10.1029/2010JE003613.
75. Eastland G. Considerations of undersea exploration of an extra-terrestrial ocean. J Acoust Soc Am. 2023;153:A281.
76. Ojha L, Wilhelm MB, Murchie SL, McEwen AS, Wray JJ, Hanley J, et al. Spectral evidence for hydrated salts in recurring slope lineae on Mars. Nat Geosci. 2015;8:829–32.
77. Vance S, Bouffard M, Choukroun M, Sotin C. Ganymede′s internal structure including thermodynamics of magnesium sulfate oceans in contact with ice. Planet Space Sci. 2014;96:62–70.
78. McCord TB, Hansen GB, Hibbitts CA. Hydrated salt minerals on Ganymede's surface: evidence of an ocean below. Science. 2001;292:1523–5.
79. Thompson SP, Kennedy H, Butler BM, Day SJ, Safi E, Evans A. Laboratory exploration of mineral precipitates from Europa's subsurface ocean. J Appl Crystallogr. 2021;54:1455–79.
80. Glein CR, Shock EL. Sodium chloride as a geophysical probe of a subsurface ocean on Enceladus: ENCELADUS' SALTY SEA. Geophys. Res. Lett. 2010;37, https://doi.org/10.1029/2010GL042446.
81. Kreysing M, Keil L, Lanzmich S, Braun D. Heat flux across an open pore enables the continuous replication and selection of oligonucleotides towards increasing length. Nat Chem. 2015;7:203–8.
82. Tervahattu H, Tuck AF, Vaida V. Chemistry in prebiotic aerosols: A mechanism for the origin of life" in Origins. In: Seckbach J. Origins Genesis, Evolution and Diversity of Life. Dordrecht: Springer; 2004, pp. 153–65.
83. Holden DT, Morato NM, Cooks RG. Aqueous microdroplets enable abiotic synthesis and chain extension of unique peptide isomers from free amino acids. Proc Natl Acad Sci USA. 2022;119:e2212642119.